Evaluation of thermal stability in spectrally selective few-layer metallo-dielectric structures for solar thermophotovoltaics

doi: 10.1016/j.jqsrt.2018.02.037

Evaluation of thermal stability in spectrally selective few-layer metallo-dielectric structures for solar thermophotovoltaics

Makoto Shimizu[1, 2], Asaka Kohiyama[1], and Hiroo Yugami[1]

[1]Graduate School of Engineering, Tohoku University, Aoba 6-6-01 Aramaki, Aoba-ku, Sendai 980-8579, Japan

[2]Univ Lyon, CNRS, INSA-Lyon, Université Claude Bernard Lyon 1, CETHIL UMR5008, F-69621, Villeurbanne, France

Corresponding author:

Makoto Shimizu

m_shimizu@energy.mech.tohoku.ac.jp

Abstract

The thermal stability of spectrally selective few-layer metallo-dielectric structures is evaluated to analyze their potential as absorber and emitter materials in solar thermophotovoltaic (STPV) systems. High-efficiency (e.g., STPV) systems require materials with spectrally selective properties, especially at high temperatures (>1273 K). Aiming to develop such materials for high-temperature applications, we propose a few-layer structure composed of a refractory metal (i.e., Mo) nanometric film sandwiched between the layers of a dielectric material (i.e., hafnium oxide,

HfO_2) deposited on a Mo bulk substrate. In vacuum conditions (<5 10^{-2} Pa), the few-layer structure shows thermal stability at 1423 K for at least 1 h. At 1473 K, the spectral selectivity was degraded. This could have been caused by the oxidation of the Mo thin film by the residual oxygen through the grain boundaries of the upper HfO_2 layer. This experiment showed the potential stability of few-layer structures for applications working at temperatures greater than 1273 K as well as the degradation mechanism of the few-layer structure. This characteristic is expected to help improve the thermal stability in few-layer structures further.

Keywords

thermal radiation; high-temperature applications; solar energy; thermophotovoltaics; multilayer structures

1. Introduction

Solar thermophotovoltaic (STPV) generation systems represent one of the solar energy conversion technologies. In these systems, thermal radiation from an emitter heated by concentrated solar power is converted into electricity by photovoltaic (PV) cells. Thus, these systems are expected to show high efficiencies

(as high as those of multijunction PV cells) via spectral matching between the emitter thermal radiation and the PV cells' external quantum efficiency (EQE). STPV systems were first suggested by Swanson in 1979 [1]. He proposed the use of silicon photodiodes with very high emitter operating temperatures (higher than 2000 K) to match the emission peak with the PV cell EQE. However, it was challenging to find materials with sufficient thermal stability at such high temperatures.

Nowadays, the required operating temperature has been reduced to practicable levels (around 1500 K) by the advancement of low-bandgap cell technologies using semiconductor compounds such as gallium antimonide (GaSb) and indium gallium arsenide (InGaAs). In addition, considerable progress has been made in designing and fabricating spectrally selective emitters and absorbers [2-5], and consequently, the reported efficiency of STPV systems has rapidly improved [6-9]. In this regard, the most recent record (6.8%) was reported by Bierman et al. Such efficiencies were achieved with a one-dimensional photonic-crystal selective emitter coupled with a tandem plasma-interference optical filter (to suppress below-bandgap photons) along with a high-quality narrow-bandgap InGaAsSb cell [10].

On the other hand, the evaluation of the stability of the system, which is essential for practical realization, has not been investigated yet. For highly stable

systems, the thermal stability of the absorber and the emitter is the key factor. Many researchers have reported spectrally selective coating technologies having good spectrally selective performances involving multilayer [11-14] and metallo-dielectric cermet [15-18] coatings. However, for systems operated at temperatures greater than 1273 K, the application of most of the reported technologies becomes difficult. Only several microstructures fabricated with refractory metals having characteristic sizes similar to the dominant thermal radiation wavelengths [19-22] have shown relatively high thermal stability at temperatures greater than 1273 K. However, it is too difficult to fabricate these microstructures on a large-area surface.

In this work, we focused on few-layer metallo-dielectric structures including a nanometric metallic film. It has been reported that this type of multilayer structure can be designed to have good spectrally selective properties based on the so-called perfect absorption phenomenon that is effective in a short wavelength range (lower than 1.5 μm) [23-25]. Further, a theoretical analysis was conducted to understand the spectrally selective emission phenomenon [26]. In our previous study, we had reported this structure for the absorber and the emitter of an STPV system, and applied it in power generation tests [9]. The structure enabled us to evaluate the performance of the system for several minutes at a high temperature of

approximately 1600 K, though we did not observe the practical applicability through long-time operation tests.

In this context, the thermal stability of the few-layer structure was evaluated in this study, aiming at a longer operation of the structure in an STPV system. Through the thermal stability test and evaluation of the degradation mechanism in this structure, we verified the thermal stability at 1423 K as well as the thermal stability for rapid heating or cooling rates, i.e. 600 K/min. It was clearly shown that degradation occurred at a temperature greater than 1473 K with this structure due to the oxidation of the metals. Avoiding oxygen diffusion through the upper dielectric layer might contribute to the improvement in the thermal stability.

2. Optical property of the few-layer structure

Considering high-temperature use, Mo and hafnium oxide (HfO_2) were the materials selected for the nanometric film and dielectric layers, respectively, owing to their high melting point (2896 and 3031 K for Mo and HfO_2, respectively). The few-layer structure was deposited by using a physical vapor deposition method. A 15-mm-square Mo plate polished to a mirror finish was used as the substrate. First, the lower HfO_2 layer was deposited by using a pulsed laser deposition (PLD) method. An argon

fluoride excimer laser (power = 60 mJ, chamber window, laser pulse frequency = 4 Hz) was used for the ablation of the target material. The processes were carried out under a pressure of 3×10^{-4} Pa and by heating the substrate at 773 K. After the deposition process, post-deposition annealing was conducted for 30 min at the same temperature as that used in the deposition process (773 K). The sample was removed from the PLD chamber and a Mo thin film was subsequently deposited with radio-frequency magnetron sputtering. The substrate temperature and the plasma power were set to 300 K and 100 W, respectively. The pressure in the chamber during the process was maintained at 7 Pa by flowing Ar. Finally, the upper HfO_2 layer was deposited by employing the same process as for the lower layer.

The spectral absorptance of the fabricated sample was measured on a VIS-NIR spectrometer (Lambda 950, Perkin Elmer) for short wavelengths (0.3–1.5 μm) and a Fourier transform infrared (FT-IR) spectrometer (FT/IR-6600, JASCO) for longer wavelengths (up to 8 μm). For both spectrometers, a 150-mm integrating sphere was used to measure the reflectance.

The fabricated structure is shown in Fig. 1 (a) as a cross-sectional image observed using transmission electron microscopy (TEM; JEM-2100, JEOL). This sample was prepared to obtain the optimum absorber property. Since diffraction

contrast patterns were observed in all layers, we concluded that all the layers were crystalized. The surface roughness slightly increased because of the columnar structure of the upper HfO_2 layer.

A step-like absorptance (or emittance) spectrum with a steep cutoff is obtained with the few-layer structure (see Fig. 1 (b)). At short wavelengths, the absorptance significantly increases in the structure. Especially, for the wavelengths 0.5 and 1.0 μm, the emittance exceeds 0.98. This enhancement from the Mo bulk property is produced by a combination of resonant thermal radiation in each HfO_2 layer [26]. Thus, the absorptance enhancement property along with its spectral bandwidth and intensity can be controlled by changing the thickness of each layer. Here, we show the optimized structure for the solar selective absorber, in which the thickness of the upper HfO_2:Mo thin film:lower HfO_2 is 60 nm:15 nm:60 nm, respectively. By increasing the thickness of both the HfO_2 layers, as 200 nm:10 nm:110 nm, the optimum emittance spectrum for the emitter (See in Ref. [9]) can be obtained. The measured spectrum is in good agreement with the simulated results. The sample has a high absorptance (exceeding 0.9) at short wavelengths and a low absorptance (lower than 0.05) at 5 μm. The slight differences observed in the 2–4 μm range may result from the differences between the optical constant values of the

prepared materials and those reported in the literature.

3. Thermal stability of the few-layer structure

The thermal stability of the structure was evaluated assuming STPV operating conditions (i.e., absorber and emitter temperatures exceeding 1273 K under vacuum). The tests were conducted in a vacuum infrared-lamp furnace for 1 h. To avoid the influence of rapid temperature changes, the samples were gradually heated or cooled to the target annealing temperature at a rate of 5 K/min. The temperature of the samples was measured with an R-type thermocouple attached at the edge of the samples. The pressure during the annealing process was kept close to 5×10^{-2} Pa. Note that the absorptance spectra were evaluated after each annealing process and not during the process.

To check the compatibility between the HfO_2 layer and the Mo substrate, the thermal stability of a HfO_2 monolayer on a Mo substrate was first evaluated. For comparison, a tungsten (W) substrate, a known refractory metal, was also employed in the test. In the case of the structure consisting of a HfO_2 layer and a Mo substrate, the absorptance spectrum remained relatively unchanged. Even after annealing at 1473 K, we did not observe any deviation from the initial deposition state as shown in Fig. 2 (a). Unlike the Mo- and HfO_2-containing structures, the absorptance spectrum of the

structure containing a HfO_2 monolayer and a W substrate is drastically affected after annealing at 1473 K (Fig. 2 (b)). Absorptance in short wavelengths (< 2 μm) is drastically decreased though the absorptance in long wavelengths (> 2 μm) is still low because the W substrate shows high reflectance. This is due to the severe detachment of the HfO_2 monolayer. In this temperature range, the three materials have relatively similar thermal expansion coefficients. Therefore, the different thermal stability values of these materials are scarcely produced by residual stresses caused by temperature changes. The strength of the chemical bonding between the substrate metal and the HfO_2 layer is proposed to explain these results, although further research is required to explain this phenomenon.

The absorptance spectra of the few-layer structure measured after each annealing temperature are shown in Fig. 3. The potential of thermal stability was verified up to 1423 K, since no change was observed in the absorptance spectrum within this temperature range. The absorptance spectrum changed drastically after annealing at 1473 K. In particular, the absorptance largely increased in the 2–3 μm range. Additionally, the absorptance peak shifted at short wavelengths.

To understand the degradation mechanism of the few-layer structure annealed at 1473 K, a cross-sectional view was observed with TEM and the x-ray

diffraction (XRD) patterns as shown in Fig. 4. The formation of the few-layer structure is catastrophically changed and some voids are observed at the substrate surface boundary between the few layers. The grain size of HfO_2 appears enlarged and the three layers, i.e., upper and lower HfO2, and Mo thin film, exist no more. From the XRD results shown in Fig. 4 (b), the clear peaks only corresponding to Mo and HfO_2 appear at the initial deposition condition. Any clear change is not seen up to 1423 K, whereas after annealing at 1473 K, peaks ascribed to molybdenum dioxide (MoO_2) are identified.

This Mo oxidation might be the main factor of spectrally selective absorption decline. In fact, HfO_2 is a more stable material than MoO_2 or molybdenum trioxide MoO_3. The enthalpy change from HfO_2 to metal is 1140 kJ/mol at 773 K, which is larger than that of MoO_2 and MoO_3 at 584 kJ/mol and 492 kJ/mol, respectively. Therefore, it is difficult to imagine the diffusion of the oxygen atom from HfO_2 to Mo, but the residual oxygen comes from the chamber. As shown in the TEM image in Fig. 1, a columnar structure is observed in the upper HfO_2 layer such that numerous vertical grain boundaries are observed among the grains. Since the test was not conducted under high-vacuum conditions (i.e., 5×10^{-2} Pa), residual oxygen in the chamber might have penetrated into the upper HfO_2 layer, passing through the grain

boundaries and oxidizing the Mo thin film. A large stress is introduced at the layer boundary by the increase of lattice volume due to oxidation. In addition, once Mo is oxidized, the melting temperature of the material drops drastically. For example, MoO_2 shows a melting point of 1373 K and MoO_3 shows a much lower value of 1068 K. Furthermore, for MoO_3, the boiling point is at 1428 K, which means sublimation of MoO_3 is occurred at 1473 K. These effects must damage the lower HfO_2 layer, and change the few-layer formation. Then, the acceleration of the oxygen diffusion thorough the grain boundaries of the HfO_2 layer causes partial oxidation of the surface of the Mo substrate. After Mo turns to MoO_3, the sublimation of the oxide causes the generation of some voids seen in Fig. 4(a). Consequently, the change of the few-layer formation and the generation of voids cause the drastic change of the absorptance spectrum.

Thus, reducing the number of grain boundaries or further coating of a dielectric layer with few grain boundaries (e.g., an amorphous film) can effectively improve the thermal stability of the few-layer structure. From the evaluation of thermal stability, it is understood that with this fabrication process and the materials used, the structure is degraded at 1473 K. However, we verified the stability up to 1423 K for at least 1 h in vacuum, which is a much higher stability

than that in the other previous spectrally selective materials. The evaluation of greater long-term stability, e.g., more than 100 h, should also be conducted to confirm the applicability to the practical operation; we could evaluate the potential of the high thermal stability in this structure. Moreover, the analysis of the degradation mechanism reveals the approach for improving the thermal stability of the few-layer structure.

4. Stability under rapid thermal cycling

In real conditions, large temperature fluctuations might occur with changes in the input power. Therefore, the absorber and the emitter have to be robust for such rapid temperature changes. We conducted a rapid thermal cycling test to evaluate the stability under rapid temperature changes. The test was conducted with a high-power solar simulator (YSS-15-C1000HR, Yamashita Denso Co.) by controlling the input power. The sample was put in a vacuum chamber with a transparent window to introduce concentrated solar energy into the sample. Part of the thermal history of this test is shown in the inset of Fig. 5. For the first condition, the temperature is raised to 1250 K. Then, it is reduced until nearly 900 K at 15-s intervals. After this quickly repeated cycle test, the temperature is increased to 1250

K again, and then reduced until 500 K at 170- s intervals. These sets of rapid thermal cycling test were repeated twice. The thermal stability was verified by comparing the absorptance spectra measured before and after annealing. The spectra were almost perfectly matched even after the test. Close values of thermal expansion coefficients of Mo and HfO_2 are helpful to achieve high stability in the case of rapid thermal cycling.

5. Conclusions

The thermal stability of few-layer spectrally selective materials was investigated for their potential role as absorbers and emitters in STPV systems. The spectrally selective property is essential in reducing radiation energy losses, especially at the high temperatures reached by STPV systems. To achieve step-function-like absorptance (emittance) spectra and high thermal stability, a few-layer structure composed of high-melting-point materials, such as Mo and HfO_2, was developed. With the proposed structure, strongly enhanced absorptance on a broad spectral range could be experimentally obtained. Compared to the compatibility of HfO_2 on the Mo and W substrates, the HfO_2 layer on the Mo substrate is more stable than that on the W substrate at 1473 K.

The thermal stability of the few-layer structure was evaluated in vacuum for 1 h. No clear change in the absorptance spectrum and XRD patterns up to 1423 K was observed. However, the performance of the structure deteriorated at 1473 K and the absorptance in the mid-IR region increases significantly due to the change in the formation of the few-layer structure.

This study demonstrates the potential of specific few-layer structures for STPV systems. Although further tests are required, these materials are expected to exhibit high thermal stability. In this study, we focus on the absorbers and emitters in STPV systems. The spectrally selective materials based on a few-layer structure are expected to contribute significantly to the improvement in the energy efficiency in other high-temperature applications.

Acknowledgment

This study was partly supported by JSPS KAKENHI Grant Number 16H02117.

References

[1] Swanson RM. Silicon photovoltaic cells in thermophotovoltaic energy conversion. Int Electron Devices Meet 1978;70–73.

[2] Licciulli A, Diso D, Torsello G, Tundo S, Maffezzoli A, Lomascolo M, Mazzer M. The challenge of high-performance selective emitters for thermophotovoltaic applications.

Semiconductor Sci Technol 2003;18:S174–S183.

[3] Zhou Z, Sakr E, Sun Y, Bermel P. Solar thermophotovoltaics: reshaping the solar spectrum. Nanophotonics 2016;5:1–21.

[4] Pfiester NA, Vandervelde TE. Selective emitters for thermophotovoltaic applications. Phys. Status Solidi A 2017;214:1600410.

[5] Dyachenko PN, Molesky S, Petrov AY, Stormer M, Krekeler T, Lang S, Ritter M, Jacob Z, Eich M. Controlling thermal emission with refractory epsilon-near-zero metamaterials via topological transitions. Nat Commun 2016;7:11809.

[6] Datas A, Algora C. Development and experimental evaluation of a complete solar thermophotovoltaic system. Prog Photovoltaics 2013;21:1025–1039.

[7] Lenert A, Bierman DM, Nam Y, Chan WR, Celanovic I, Soljacic M, Wang EN. A nanophotonic solar thermophotovoltaic device. Nat Nano 2014;9:126–130.

[8] Ungaro C, Gray SK, Gupta MC. Solar thermophotovoltaic system using nanostructures. Opt Express 2015;23:A1149–A1156.

[9] Kohiyama A, Shimizu M, Yugami H. Unidirectional radiative heat transfer with a spectrally selective planar absorber/emitter for high-efficiency solar thermophotovoltaic systems. Appl Phys Express 2016;9:112302.

[10] Bierman DM, Lenert A, Chan WR, Bhatia B, Celanović I, Soljačić M, Wang EN. Enhanced photovoltaic energy conversion using thermally based spectral shaping. Nat Energy 2016;1:16068.

[11] Barshilia HC, Selvakumar N, Rajam KS, Sridhara Rao DV, Muraleedharan K. Deposition and characterization of TiAlN/TiAlON/Si_3N_4 tandem absorbers prepared using reactive direct current magnetron sputtering. Thin Solid Films 2008;516:6071–6078.

[12] Barshilia HC, Selvakumar N, Vignesh G, Rajam KS, Biswas A. Optical properties and thermal stability of pulsed-sputter-deposited Al_xO_y/Al/Al_xO_y multilayer absorber coatings. Sol Energy Mater Sol Cells 2009;93:315–323.

[13] Selvakumar N, Manikandanath NT, Biswas A, Barshilia HC, Design and fabrication of highly thermally stable HfMoN/HfON/Al_2O_3 tandem absorber for solar thermal power

generation applications. Sol Energy Mater Sol Cells 2012;102:86–92.

[14] Rebouta L, Sousa A, Andritschky M, Cerqueira F, Tavares CJ, Santilli P, Pischow K. Solar selective absorbing coatings based on AlSiN/AlSiON/$AlSiO_y$ layers. Appl Surf Sci 2015;356:203–212.

[15] Zhang QC, Yin YB, Mills DR. High efficiency Mo-Al_2O_3 cermet selective surfaces for high-temperature application. Sol Energy Mater Sol Cells 1996;40:43–53.

[16] Nejati MR, Fathollahi V, Khalaji Asadi M. Computer simulation of the optical properties of high-temperature cermet solar selective coatings. Sol Energy 2005;78:235–241.

[17] Gaouyat L, He Z, Colomer JF, Lambin P, Mirabella F, Schryvers D, Deparis O. Revealing the innermost nanostructure of sputtered $NiCrO_x$ solar absorber cermets. Sol Energy Mater Sol Cells 2014;122:303–308.

[18] Zheng L, Zhou F, Zhou Z, Song X, Dong G, Wang M, Diao X. Angular solar absorptance and thermal stability of Mo–SiO2 double cermet solar selective absorber coating, Sol Energy 2015;115:341–346.

[19] Sai H, Kanamori Y, Yugami H. High-temperature resistive surface grating for spectral control of thermal radiation. Appl Phys Lett, 2003;82:1685–1687.

[20] Kusunoki F, Kohama TK, Hiroshima T, Fukumoto S, Takahara J, Kobayashi T. Narrow-band thermal radiation with low directivity by resonant modes inside tungsten microcavities. Jpn J Appl Phys Part 1 2004;43:5253–5258.

[21] Rinnerbauer V, Yeng YX, Chan WR, Senkevich JJ, Joannopoulos JD, Soljacic M, Celanovic I. High-temperature stability and selective thermal emission of polycrystalline tantalum photonic crystals. Opt Express, 2013;21:11482–11491.

[22] Garín M, Hernández D, Trifonov T, Alcubilla R. Three-dimensional metallo-dielectric selective thermal emitters with high-temperature stability for thermophotovoltaic applications. Sol Energy Mater Sol Cells 2015;134:22–28.

[23] Kats MA, Sharma D, Lin J, Genevet P, Blanchard R, Yang Z, Qazilbash MM, Basov DN, Ramanathan S, Capasso F. Ultra-thin perfect absorber employing a tunable phase

change material. Appl Phys Lett 2012;101:221101.

[24] Kats MA, Blanchard R, Genevet P, Capasso F. Nanometre optical coatings based on strong interference effects in highly absorbing media. Nat Mater 2013;12:20–24.

[25] Foley JJ, Ungaro C, Sun KY, Gupta MC, Gray SK. Design of emitter structures based on resonant perfect absorption for thermophotovoltaic applications. Opt Express 2015;23:A1373–A1387.

[26] Blandre E. Thermal radiation at the nanoscale: nearfield and interference effects in few-layer structures and on the electrical performances of thermophotovoltaic devices. Doctoral Thesis, INSA Lyon, France, 2016.

Figures

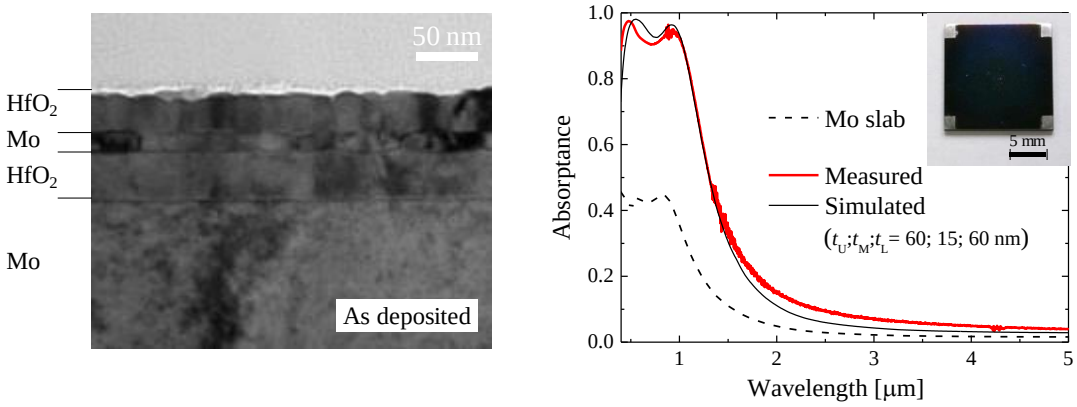

Fig. 1 (a) Cross-sectional image of the fabricated as-deposited few-layer structure, observed with a TEM. (b) Measured and simulated absorptance spectra of the structure (solid red and black lines, respectively) at room temperature compared to that of bulk Mo (dashed black line). Inserted figure shows a picture of the sample.

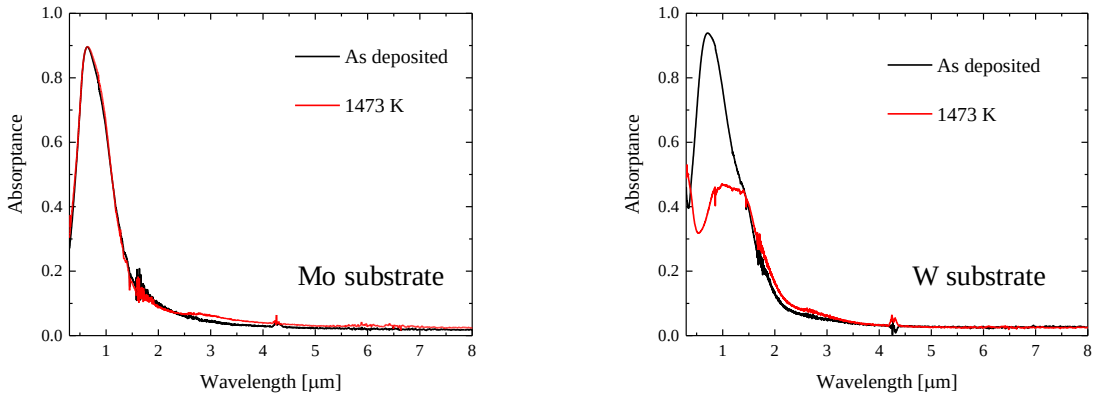

Fig. 2 (a) Measured absorptance spectra of the single HfO_2 layer on Mo substrate as-deposited (black line) and after annealing at 1473 K for 1 h (red line). (b) Measured absorptance spectra of the single HfO_2 layer on W substrate as-deposited (black line) and after annealing at 1473 K for 1 h (red line).

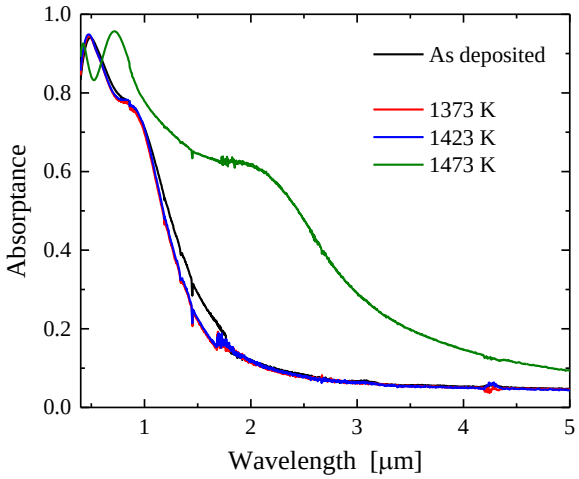

Fig. 3 Measured absorptance spectra of the few-layer structure as-deposited (black line) and after annealing at 1373 K (red line), 1423 K (blue line), and 1473 K (green

line) for 1h.

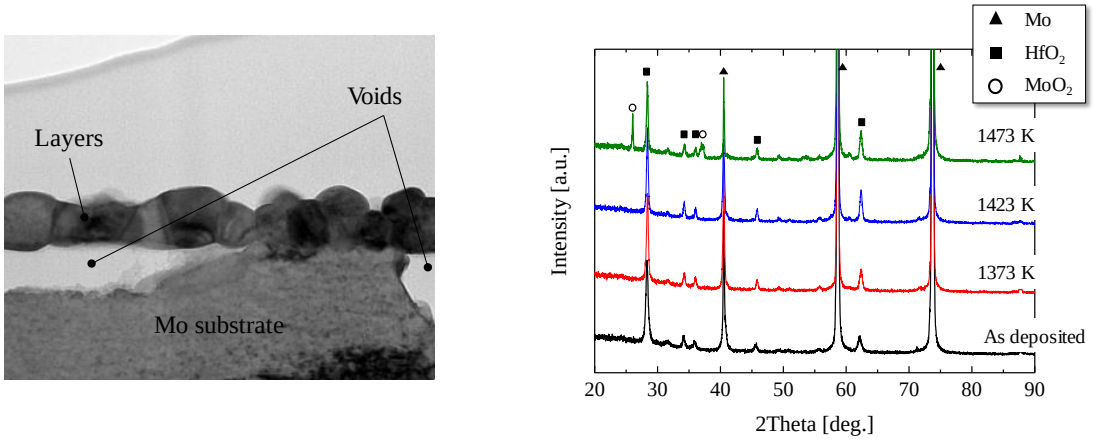

(a) (b)

Fig. 4 (a) Cross-sectional image of the fabricated few-layer structure after annealing at 1473 K for 1 h, observed with TEM. (b) XRD patterns of the as-deposited few-layer structure and after the different annealing processes.

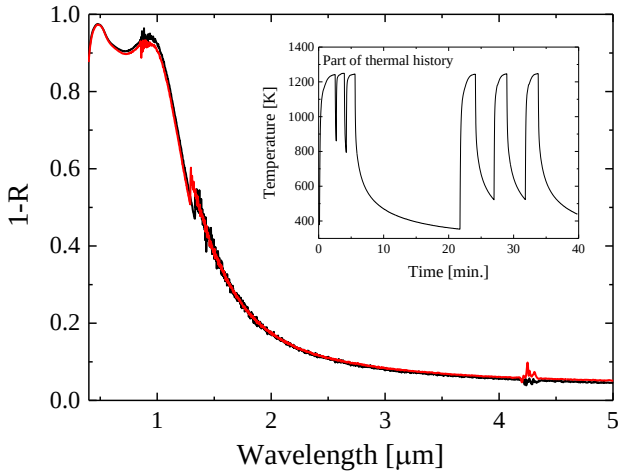

Fig. 5 Measured absorptance spectra of as-deposited few-layer structure (black) and

after the whole thermal cycling test (red). The inserted graph shows a part of the thermal history of the test.